

## Supercooling transition in phase separated manganite thin films: An electrical transport study

Sandeep Singh, Pawan Kumar, P. K. Siwach, Pawan Kumar Tyagi, and H. K. Singh

Citation: [Applied Physics Letters](#) **104**, 212403 (2014); doi: 10.1063/1.4880725

View online: <http://dx.doi.org/10.1063/1.4880725>

View Table of Contents: <http://scitation.aip.org/content/aip/journal/apl/104/21?ver=pdfcov>

Published by the [AIP Publishing](#)

---

### Articles you may be interested in

[Anisotropic resistivities in anisotropic-strain-controlled phase-separated  \$\text{La}\_{0.67}\text{Ca}\_{0.33}\text{MnO}\_3/\text{NdGaO}\_3\(100\)\$  films](#)  
Appl. Phys. Lett. **103**, 072407 (2013); 10.1063/1.4818636

[Enhanced magnetic refrigeration capacity in phase separated manganites](#)  
Appl. Phys. Lett. **95**, 092506 (2009); 10.1063/1.3204694

[Magnetic separation and inelastic tunneling in self-doped manganite films](#)  
J. Appl. Phys. **106**, 043908 (2009); 10.1063/1.3197855

[Studies on the cluster sizes in the mixed-phase thin films](#)  
Appl. Phys. Lett. **90**, 032508 (2007); 10.1063/1.2432945

[Influence of different substrates on phase separation in  \$\text{La}\_{1-x-y}\text{Pr}\_y\text{Ca}\_x\text{MnO}\_3\$  thin films](#)  
J. Appl. Phys. **99**, 08S901 (2006); 10.1063/1.2162050

---

A promotional banner for the 2014 Special Topics in AIP Applied Physics Letters. The banner has an orange background with a white border. At the top, the text '2014 Special Topics' is written in a large, white, sans-serif font. Below this text, there are five circular icons, each containing a different material structure and a label: 'PEROVSKITES' (red and black geometric shapes), '2D MATERIALS' (blue and red hexagonal lattice), 'MESOPOROUS MATERIALS' (green and yellow porous structure), 'BIOMATERIALS/ BIOELECTRONICS' (yellow and black structure), and 'METAL-ORGANIC FRAMEWORK MATERIALS' (brown and black structure). At the bottom left, the 'AIP | APL Materials' logo is displayed. At the bottom right, a red banner with white text says 'Submit Today!'.

# Supercooling transition in phase separated manganite thin films: An electrical transport study

Sandeep Singh,<sup>1,2</sup> Pawan Kumar,<sup>1,3</sup> P. K. Siwach,<sup>1</sup> Pawan Kumar Tyagi,<sup>2</sup> and H. K. Singh<sup>1,a)</sup>

<sup>1</sup>National Physical Laboratory (Council of Scientific and Industrial Research), Dr. K. S. Krishnan Marg, New Delhi 110012, India

<sup>2</sup>Department of Applied Physics, Delhi Technological University, Delhi 110042, India

<sup>3</sup>Inter-University Accelerator Centre, Aruna Asaf Ali Marg, New Delhi 110067, India

(Received 19 March 2014; accepted 18 May 2014; published online 29 May 2014)

The impact of variation in the relative fractions of the ferromagnetic metallic and antiferromagnetic/charge ordered insulator phases on the supercooling/superheating transition in strongly phase separated system,  $\text{La}_{5/8-y}\text{Pr}_y\text{Ca}_{3/8}\text{MnO}_3$  ( $y \approx 0.4$ ), has been studied employing magnetotransport measurements. Our study clearly shows that the supercooling transition temperature is non-unique and strongly depends on the magneto-thermodynamic path through which the low temperature state is accessed. In contrast, the superheating transition temperature remains constant. The thermo-magnetic hysteresis, the separation of the two transitions and the associated resistivity, all are functions of the relative fraction of the coexisting phases. © 2014 AIP Publishing LLC. [<http://dx.doi.org/10.1063/1.4880725>]

Phase separation (PS) is believed to be the key ingredient of the physics of doped rare earth manganites.<sup>1–3</sup> It dominates the composition-temperature ( $x$ - $T$ ) diagram of intermediate and low bandwidth manganites like  $\text{Nd}_{1-x}\text{Sr}_x\text{MnO}_3$ ,<sup>3,4</sup>  $\text{Sm}_{1-x}\text{Sr}_x\text{MnO}_3$ ,<sup>5,6</sup> and  $\text{La}_{1-x-y}\text{Pr}_y\text{Ca}_x\text{MnO}_3$ .<sup>7–10</sup> Amongst these materials,  $\text{La}_{1-x-y}\text{Pr}_y\text{Ca}_x\text{MnO}_3$  has emerged as the prototypical phase separated system and its different variants like bulk single crystal, polycrystals, and thin films have been investigated.<sup>7–16</sup> The strong nature of the phase separation has been established by the observation of (i) strong divergence of the zero field cooled (ZFC) and field cooled warming (FCW) magnetization, (ii) pronounced hysteresis between the field cooled cool (FCC) and FCW magnetization, and (iii) prominent thermomagnetic hysteresis in the temperature and magnetic field ( $H$ ) dependent resistivity ( $\rho$ ) measured in cooling-warming cycles.<sup>7–16</sup> A study by Uehara *et al.*<sup>7</sup> has shown the coexistence of sub-micrometer scale ferromagnetic metallic (FMM) and antiferromagnetic/charge ordered insulator (AFM/COI) clusters and that the latter is explicit in magnetotransport measurements only at  $y \geq 0.3$ . Consequently, the electrical transport becomes percolative, which is evidenced by huge residual resistivity ( $\rho_0$ ) for  $y \approx 0.4$  in the metallic regime.<sup>7</sup> The study of Ghivelder and Parisi<sup>8</sup> on bulk  $\text{La}_{5/8-y}\text{Pr}_y\text{Ca}_{3/8}\text{MnO}_3$  ( $y \approx 0.4$ ) has shown that COI phase appears at  $T_{\text{CO}} \sim 230$  K and subsequently acquires AFM and FM spin order  $T_N \sim 180$  and  $T_C \sim 80$  K, respectively. Due to the rapid spatial and temporal variations in the relative fraction of the FMM and AFM/COI phases, large relaxation effects are also observed.<sup>8</sup> Further, the theoretical study by Ghivelder and Parisi<sup>8</sup> has predicted that interplay between temperature and separation of the system from equilibrium could create multiple blocked states. Sharma *et al.*<sup>9</sup> studied the same material and have established the existence of a liquid like magnetic phase in the phase separated regime, which

transforms cooperatively to a randomly frozen glass like phase at low temperature. The frozen glass like phase (termed as strain glass) is believed to arise from the presence of martensitic accommodation strain.<sup>9</sup> Wu *et al.*<sup>10</sup> have demonstrated that in  $\text{La}_{5/8-y}\text{Pr}_y\text{Ca}_{3/8}\text{MnO}_3$  ( $y \approx 0.4$ ) thin films the magnetic liquid like phase exhibits a supercooled glass transition. This glass transition is believed to arise due to the presence of the accommodation strain caused by distinct structural symmetries of FMM and AFM/COI phases. Their study has also provided evidence in favour of the non-ergodic nature of the magnetic liquid. Wu *et al.*<sup>10</sup> have shown that non-ergodicity appears when the long range cooperative strain interactions hinder the cooperative dynamic freezing of the first-order AFM/COI-FMM transition.<sup>9,10</sup>

The FCC-FCW and thermoresistive hysteresis are regarded as signatures of supercooling and superheating transition of the magnetic liquid formed by competing FMM and AFM phases in the presence of martensitic of accommodation strain and long range cooperative strain interactions.<sup>8–10</sup> Despite the exhaustive investigations on different variants of the  $\text{La}_{1-x-y}\text{Pr}_y\text{Ca}_x\text{MnO}_3$ , the nature of the supercooling/superheating transitions, e.g., their dependence on relative fractions of FMM and AFM phases has not been probed through electrical transport measurements. The different relative fractions of the FM/AFM phases at the beginning of the magneto-thermodynamic process are expected to lead to different thermodynamic paths and yield different supercooling transition temperatures. Hence, it is important to investigate the signature of different magneto-thermodynamic paths in electrical transport. In this Letter, we report the electrical transport studies on  $\text{La}_{5/8-y}\text{Pr}_y\text{Ca}_{3/8}\text{MnO}_3$  ( $y \approx 0.4$ ) epitaxial thin films. Our results demonstrate that of the two observed insulator-metal transitions (IMTs), the lower one caused by the supercooling of a magnetic liquid is non-unique, while the upper one remains constant.

The  $\text{La}_{5/8-y}\text{Pr}_y\text{Ca}_{3/8}\text{MnO}_3$  ( $y \approx 0.4$ ) thin films were grown by RF magnetron sputtering of a stoichiometric (2 in.)

<sup>a)</sup> Author to whom correspondence should be addressed. Electronic mail: hks65@nplindia.org.

target in 200 mTorr of Ar + O<sub>2</sub> (80 + 20) mixture on single crystal (001) SrTiO<sub>3</sub> (STO) substrates maintained at  $\sim 800^\circ\text{C}$ . The lattice mismatch ( $\varepsilon$ ) between the target and substrate is  $\approx -1.93\%$  ( $\varepsilon = (a_t - a_s) \times 100 / a_s$  where  $a_t$  and  $a_s$  are the lattice parameters of the bulk target and substrate, respectively) and hence the strain is tensile. In order to achieve optimum oxygen content, the films were annealed at  $\approx 900^\circ\text{C}$  for 10 h in flowing oxygen.

The film thickness estimated from the X-ray reflectivity data is  $\sim 41\text{ nm}$ . The high resolution X-ray diffraction (HRXRD;  $2\theta$ - $\omega$  scan,  $\phi$ -scan, and  $\omega$ - $2\theta$  scan) confirmed the epitaxial nature of the films and also showed that the film is under tensile strain. The significantly reduced out-of-plane lattice constant of the film is  $a_f = 3.7988\text{ \AA}$  ( $a_{\text{bulk}} = 3.831\text{ \AA}$ ), which confirms the presence of appreciable tensile strain. The occurrence of the step-terrace features in the surface topography further confirms the epitaxial nature of the films.

The temperature dependent magnetization (M-T) was measured using ZFC, FCC, and FCW protocols. The ZFC, FCC, and FCW data plotted in Fig. 1 show several interesting features, viz., (i) huge irreversibility in the ZFC and FCW curves, (ii) pronounced hysteresis between the FCC and FCW curves, (iii) reversible behavior of FCC and FCW curves below  $T \approx 26\text{ K}$ , (iv) a peak in the FCW M-T around  $T_P \sim 43\text{ K}$ , and (v) sharp drop in ZFC M-T curve around  $T_P$ . The ZFC-FCW irreversibility, which is distinct from that of a representative spin glass state,<sup>17</sup> is invariably observed in phase separated manganites as a signature of cluster glass state.<sup>18–20</sup> The cluster glass state is prevalent in the intermediate bandwidth manganites having  $x \sim 1/2$ <sup>18</sup> or over a wide range of divalent doping ( $x$ ) in low bandwidth manganites<sup>19,20</sup> and originates due to the coexistence of FMM and AFM/COI phases below the Neel temperature  $T_N$ . The sharp drop in the ZFC curve observed at temperature marked  $T_P$  is a signature of cluster freezing. The prominent FCC-FCW hysteresis is signature of the different magneto-thermodynamics of the system in the two protocols and arises due to the global frustration created by the AFM/COI phase that increases the energy

of the system and also the degeneracy of the energy minima. Hence, the origin of the non-ergodicity is traceable to the AFM/COI phase, which alone can create frustration. The low temperature ( $T < 26\text{ K}$ ) reversible behavior of the FCC and FCW has been regarded as a signature of an equilibrium state attained in the FCC protocol by Ghivelder and Parisi<sup>9</sup> and could be related to the blocking of system or freezing of the cluster glass. The increase in magnetization at  $T > 26\text{ K}$  is the signature of unblocking of the system states, and hence, the peak at  $T_P \sim 43\text{ K}$  can be regarded as the onset of cluster freezing.

The FM transition, determined from the derivative of M-T data (inset of Fig. 1), occurs at  $T_C \approx 117\text{ K}$ ,  $T_C^C \approx 63\text{ K}$ , and  $T_C^W \approx 120\text{ K}$  in the ZFC, FCC, and FCW protocols, respectively. The protocol dependence of FM transition temperature could be regarded as evidence of non-ergodicity. A significantly lower value of FM transition temperature in FCC protocol can be considered as a consequence of supercooling,<sup>10</sup> whereas the FCW FM transition at  $T_C^W \approx 120\text{ K}$  can be taken as the equilibrium FM transition. The COI and AFM transitions are not explicit in the M-T data. This could be attributed to defect induced quenching of AFM/COI in thin film form.<sup>12–16</sup>

The drastic difference between the FM transition temperatures in FCC and FCW protocols can be understood in terms of the accommodation strain arising due to the distinct structural symmetry of the coexisting FM (pseudocubic) and AFM/COI (orthorhombic) phases.<sup>11,21</sup> The accommodation strain and the magnetic frustration induced by AFM order would create multiple minima in the energy landscape of the system and hence could hinder the nucleation of the equilibrium low temperature state. Such a scenario in turn could give rise to a liquid like magnetic phase.<sup>9</sup> The electrical transport characteristics of the magnetic liquid phase should depend on the relative fractions of FM and AFM/COI phases at the instant from where the low temperature state is arrived. Hence, IMT temperature ( $T_{\text{IM}}$ ) corresponding to liquid like magnetic phase should be non-unique and depend on the magneto-thermodynamic path used to access the low temperature state of the system. In view of the variation in the relative fractions of FM and AFM/COI phases across  $T_C^W$ ,  $T_{\text{IM}}$  must be a function of the temperature ( $T^*$ ) corresponding to the initial state of the magneto-thermodynamic process. This was experimentally verified by temperature dependent resistivity ( $\rho$ -T) measurement using a protocol in which the magneto-thermodynamic cycle was started from a temperature ( $T^*$ ), which was achieved by cooling the sample from room temperature to  $6\text{ K}$  and subsequent warming up to  $T^*$ .  $\rho$ -T was measured during cooling and warming employing the cycle  $T^* \rightarrow 6\text{ K} \rightarrow T$  ( $T > T_{\text{IM}}^W$ ) at  $H = 0$  and  $H = 10\text{ kOe}$ . In view of the M-T data present above, it is obvious that each  $T^*$  corresponds to a distinct ratio of FMM and AFM/COI phases. Here, we would like to mention that the impact of thermal cycling on the thermoresistive hysteresis, IMT, and peak resistivity in phase separated manganites has also been studied previously.<sup>22,23</sup> Mahendiran *et al.*,<sup>22</sup> employing a protocol of measurement different from the one used in the present case, have shown that (i) the resistivity close to and just below IMT is unstable, (ii) the resistivity increases with respect to thermal cycling, and (iii) the  $\rho$ -T

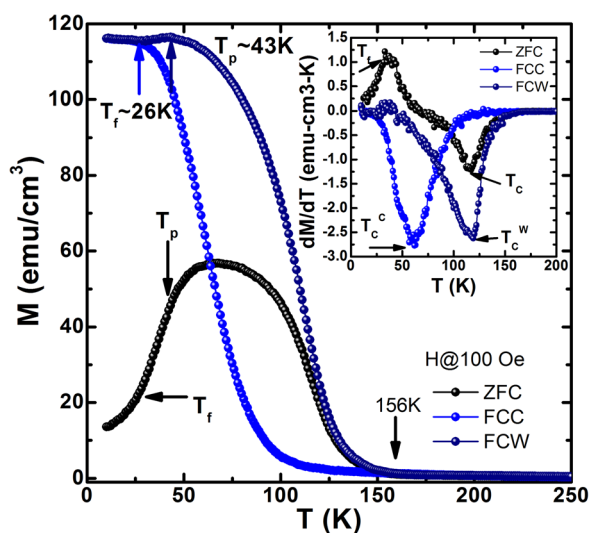


FIG. 1. The temperature dependence of ZFC, FCC, and FCW magnetization measured at  $H = 100\text{ Oe}$ . The inset shows the temperature derivative of the ZFC, FCC, and FCW curves. Various transitional features are marked in the figure.

behaviour is hysteretic even when the sample is warmed from just above the IMT. These studies have outlined the important role of strain and percolation in electrical transport in phase separated manganites.

The full cycle (300 K  $\rightarrow$  6 K  $\rightarrow$  300 K)  $\rho$ -T taken during cooling and warming (cooling and warming rate 1 K/min) is plotted in Fig. 2(a). In the cooling cycle IMT occurs at  $T_{IM}^C \approx 64$  K, where  $\rho$  drops by more than four orders of magnitude within a narrow temperature window. This is generally attributed to the abrupt enhancement in the FMM fraction at the cost of the AFM/COI.<sup>3</sup> During the warming cycle, the  $\rho$ -T curve shows a minimum at  $T_m \approx 45$  K and IMT appears at  $T_{IM}^W \approx 123$  K. The rapid rise in resistivity just below  $T_{IM}^W$  corresponds to the enhanced fraction of the AFM/COI. The huge thermo-resistive hysteresis in the  $\rho$ -T curve and large  $\Delta T_{IM} = T_{IM}^W - T_{IM}^C \approx 59$  K unravels the strongly phase separated nature of the system. The  $T_{IM}^C$  almost coincides with the FCC  $T_C^C \approx 63$  K, while  $T_{IM}^W \approx 123$  K is very close to  $T_C^W \approx 120$  K. It is believed that the drastically lowered  $T_{IM}^C$  and  $T_C^C$  is caused by supercooling of the phase separated magnetic liquid consisting of FMM and AFM/COI sub-lattices.<sup>7-13</sup>

The zero field cooling and warming cycle  $\rho$ -T data acquired after cooling from different  $T^*$  is plotted in Figs. 2(b)–2(f). When the film is cooled down from  $T^* \approx 97$  K, IMT not is observed in the cooling cycle. However, for all higher values of  $T^*$ , IMT appears in the cooling cycles at temperature that we denote by which we denote by  $T_{IM}^{C*}$ . The value of  $T_{IM}^{C*}$  for  $T^* \approx 105$  K, 113 K, 117 K, 122 K, and 143 K are observed to be 103 K, 95 K, 88 K, 79 K, and 69 K, respectively. For values of  $T^* \geq 170$  K, the  $T_{IM}^{C*}$  saturates to

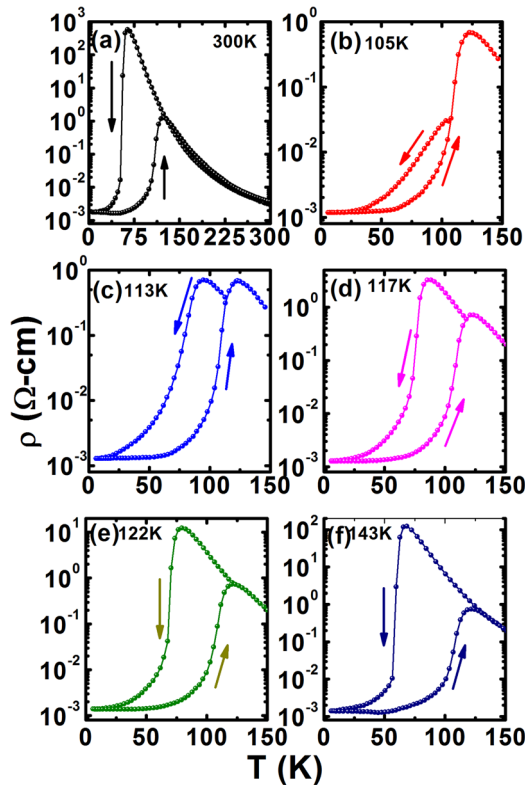


FIG. 2. Temperature dependence of resistivity measured in zero magnetic field in cooling and warming cycles after initial cooling to 6 K and subsequent warming to different  $T^*$ .

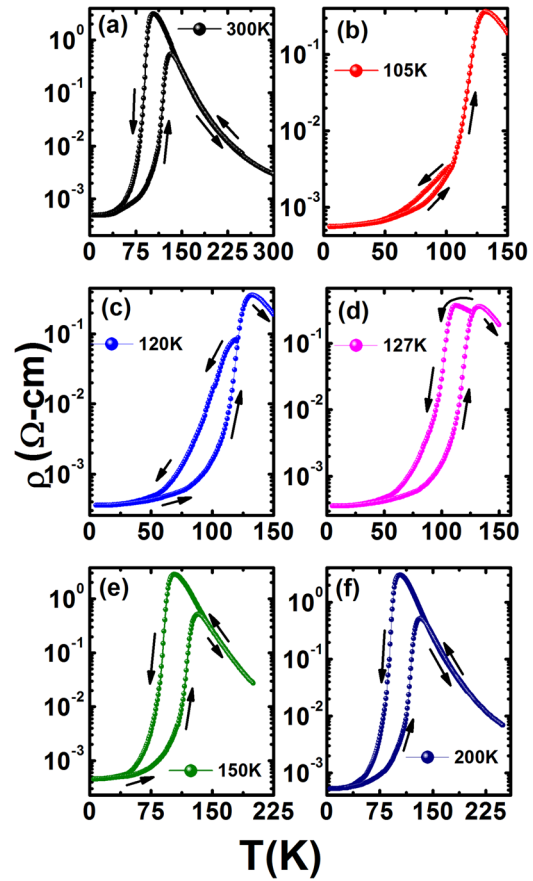


FIG. 3. Temperature dependence of resistivity measured in a magnetic field of  $H = 10$  kOe in cooling and warming cycles after initial cooling to 6 K and subsequent warming to different  $T^*$ .

$T_{IM}^C \approx 64$  K, the full cycle value. Interestingly, the warming cycle IMT,  $T_{IM}^W$  remains independent of  $T^*$ . The field ( $H = 10$  kOe) cooling and warming cycle  $\rho$ -T data acquired after cooling from different  $T^*$  are plotted in Fig. 3. The full cycle  $\rho$ -T shows  $T_{IM}^C \approx 104$  K and  $T_{IM}^W \approx 133$  K. At  $H = 10$  kOe, the cooling cycle IMT shows an increase of 40 K, which, however, is only 10 K in the warming cycle. This could be attributed to the substantial suppression of AFM induced frustration in the phase separated regime. For  $T^* = 105$  K, no IMT was observed in cooling cycle, while in warming cycle IMT was observed at  $T_{IM}^W \approx 133$  K. The absence of IMT for  $T^* = 105$  K shows that at this temperature the film has a dominant FMM fraction. For higher  $T^*$  ( $< T_{IM}^W$ ), e.g., 120 K and 127 K, IMT occurs at  $T_{IM}^{C*} \sim 119$  K and 112 K, respectively, was observed in the cooling cycle but the warming cycle IMT remained constant at  $T_{IM}^W \approx 133$  K (Fig. 3). For further higher values of  $T^* = 150$  K, 200 K, and 300 K, both  $T_{IM}^{C*}$  and  $T_{IM}^W$  remain constant at 104 K and 133 K, respectively. The variation of  $T_{IM}^{C*}$  and the corresponding peak resistivity measured in the cooling cycle ( $\rho_{IMC}$ ) are plotted in Figs. 4(a) and 4(b), respectively. From Fig. 4, it is clear that the relative fraction of the FMM and AFM phases also controls the resistivity ( $\rho_{IMC}$ ) at  $T_{IM}^{C*}$ . The difference of more than two orders of magnitude in  $\rho_{IMC}$  measured at  $H = 0$  and 10 kOe clearly reflects the colossal magnetoresistance effect. Another interesting feature seen in the zero field warming  $\rho$ -T data is the appearance (disappearance) of resistivity minimum  $\rho_m$  ( $T_m$ )



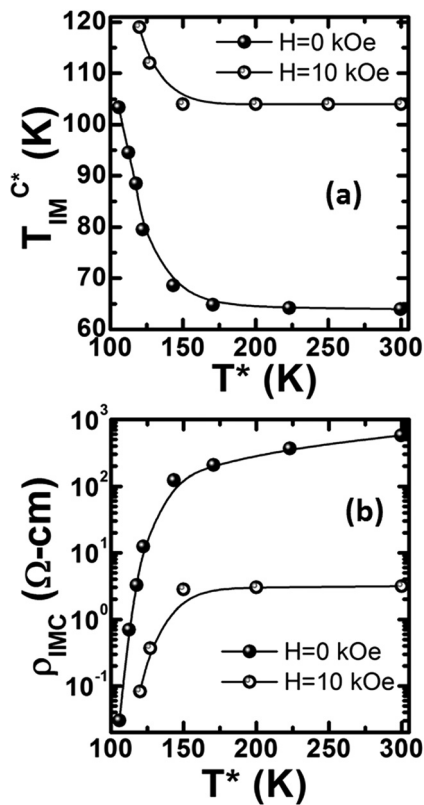


FIG. 4. (a) The variation of the  $T_{IM}^{C*}$  as a function of the characteristic temperature  $T^*$  measured at  $H=0$  and 10 kOe. (b) The variation of the peak resistivity measured in the cooling cycle as a function of  $T^*$ .

for all  $T^* \geq 143$  K ( $\leq 122$  K). In the measurements carried out at  $H=10$  kOe, no  $\rho_m$  ( $T_m$ ) is observed at all. When the sample is cooled from a  $T^*$  at which the either FMM is in minority or absent,  $T_{IM}^{C*}$  saturates to the lowest value  $T_C^C \approx 64$  K and the resistivity minimum reappears. This clearly shows that the AFM fraction is a key to the occurrence of resistivity minimum and is probably related to the freezing of the strain glass state.

The existence of different  $T_{IM}^{C*}$  for different  $T^* < T_{IM}^W$  is an unambiguous signature of non-ergodicity, which in the present case arises due the existence of different energy configuration for each magneto-thermodynamic path. At  $T^* > T_{IM}^W$ , the fraction of FMM (AFM/COI) phase decreases (increases), leading to dilution of the competitive phase coexistence tendency and therefore no modulation of the IMT. The results presented above clearly show that the supercooling transition temperature is strongly dependent on  $T^*$ , i.e., on the relative fraction of the two coexisting phases (FMM and AFM/COI) and hence the degree of magnetic

frustration at the temperature from where the system is cooled down to access the low temperature state.

To conclude, we have shown that the electrical transport in a strongly phase separated manganite thin film is extremely sensitive to the relative fraction of the coexisting FMM and AFM/COI phases and has inherent non-ergodicity. The phase separation tendency is weakened when the fraction of AFM/COI phase is reduced. The supercooling insulator-metal transition is non-unique and depends on the relative fractions of the FMM and AFM phases at the start of the magneto-thermodynamic process. In contrast, the superheating transition has equilibrium characteristic and remains independent of the ratio of the two ordered phases.

Authors are grateful to Professor R. C. Budhani for his persistent encouragement. Dr. Anurag Gupta and Dr. V. P. S. Awana are thankfully acknowledged for magnetic (MPMS-DST facility) and magnetotransport measurement, respectively.

<sup>1</sup>E. Dagotto, T. Hotta, and A. Moreo, *Phys. Rep.* **344**, 1 (2001).

<sup>2</sup>E. Dagotto, *New J. Phys.* **7**, 67 (2005).

<sup>3</sup>Y. Tokura, *Rep. Prog. Phys.* **69**, 797 (2006).

<sup>4</sup>H. Kuwahara, Y. Tomioka, A. Asamitsu, Y. Moritomo, and Y. Tokura, *Science* **270**, 961 (1995).

<sup>5</sup>Y. Tomioka, H. Hiraka, Y. Endoh, and Y. Tokura, *Phys. Rev. B* **74**, 104420 (2006).

<sup>6</sup>M. K. Srivastava, A. Kaur, K. K. Maurya, V. P. S. Awana, and H. K. Singh, *Appl. Phys. Lett.* **102**, 032402 (2013).

<sup>7</sup>M. Uehara, S. Mori, C. H. Chen, and S.-W. Cheong, *Nature* **399**, 560 (1999).

<sup>8</sup>L. Ghivelder and F. Parisi, *Phys. Rev. B* **71**, 184425 (2005).

<sup>9</sup>P. A. Sharma, S. B. Kim, T. Y. Koo, S. Guha, and S.-W. Cheong, *Phys. Rev. B* **71**, 224416 (2005).

<sup>10</sup>W. Wu, C. Israel, N. Hur, S. Park, S.-W. Cheong, and A. de Lozanne, *Nature Mater.* **5**, 881 (2006).

<sup>11</sup>V. Podzorov, B. G. Kim, V. Kiryukhin, M. E. Gershenson, and S.-W. Cheong, *Phys. Rev. B* **64**, 140406R (2001).

<sup>12</sup>T. Dhakal, J. Tosado, and A. Biswas, *Phys. Rev. B* **75**, 092404 (2007).

<sup>13</sup>H. Jeon and A. Biswas, *Phys. Rev. B* **88**, 024415 (2013).

<sup>14</sup>T. Z. Ward, S. Liang, K. Fuchigami, L. F. Yin, E. Dagotto, E. W. Plummer, and J. Shen, *Phys. Rev. Lett.* **100**, 247204 (2008).

<sup>15</sup>V. G. Sathe, A. Ahlawat, R. Rawat, and P. Chaddah, *J. Phys. Condens. Matter* **22**, 176002 (2010).

<sup>16</sup>S. Singh, M. R. Fitzsimmons, H. Jeon, A. Biswas, and M. E. Hawley, *Appl. Phys. Lett.* **101**, 022404 (2012).

<sup>17</sup>J. A. Mydosh, *Spin Glasses: An Experimental Introduction*, 2nd ed. (Taylor & Francis, London, 1993).

<sup>18</sup>R. Prasad, M. P. Singh, P. K. Siwach, A. Kaur, P. Fournier, and H. K. Singh, *Appl. Phys. A* **99**, 823 (2010).

<sup>19</sup>V. Agarwal, R. Prasad, M. P. Singh, P. K. Siwach, A. Srivastava, P. Fournier, and H. K. Singh, *Appl. Phys. Lett.* **96**, 052512 (2010).

<sup>20</sup>M. K. Srivastava, P. K. Siwach, A. Kaur, and H. K. Singh, *Appl. Phys. Lett.* **97**, 182503 (2010).

<sup>21</sup>P. Littlewood, *Nature* **399**, 529–530 (1999).

<sup>22</sup>R. Mahendiran, A. Maignan, M. Hervieu, C. Martin, and B. Raveau, *J. Appl. Phys.* **90**, 2422 (2001).

<sup>23</sup>J. Fan, L. Pi, and Y. Zhang, *J. Magn. Magn. Mater.* **307**, 186 (2006).